Electronic Supplementary Material (ESI) for Faraday Discussions.
This journal is © The Royal Society of Chemistry 2019

Performance of Enhanced DuBois Type Water Reduction Catalysts (WRC) in Artificial Photosynthesis – Effects of Various Proton Relays during Catalysis

Wolfgang Viertl,[a] Johann Pann,[a] Richard Pehn,[a] Helena Roithmeyer,[a] Marvin Bendig,[a] Alba Rodríguez-Villalón,[b] Raphael Bereiter,[a] Max Heiderscheid,[a] Thomas Müller,[a] Xia Zhao,[c] Thomas Hofer[a], Mark E. Thompson[d], Shuyang Shi[d] and Peter Brueggeller[a,*]

[a] *University of Innsbruck, Centrum for Chemistry and Biomedicine, Institute of General, Inorganic and Theoretical Chemistry, Innrain 82, 6020 Innsbruck, Austria*

[b] *Complutense University of Madrid, Avda. de Séneca, 2, Ciudad Universitaria, 28040 Madrid, Spain*

[c] *Northwest University, Taibai Road 229, Beilin District, Xi'an 710069, P. R. China*

[d] *University of Southern California, Irani Chair of Chemistry Department of Chemistry, Chemical Engineering and Materials Science Seeley G. Mudd Bldg. 3620 McClintock Ave. Los Angeles, CA 90089-1062*

Results and discussion

Influence of pendant amines as proton relays in hydrogen production

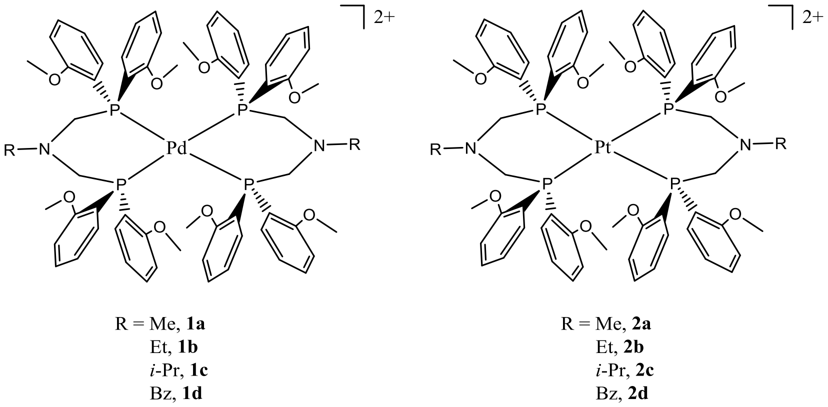

*Figure 1 Homoleptic palladium **1a-d** and platinum complexes **2a-d** with methyl-, ethyl-,* iso-*propyl and benzyl substitutions at the amine site*

In the case of the platinum series (see Figure 1, compounds **2a-d**) the methylated compound **2a** shows the best result of 10.7 turn-overs within 24 hours (see Table 1). This can be explained by the small substituent and the low steric pressure. The smaller the amine alkylation is, the easier protons can be transferred from the proton relay to the active metal centre. Interestingly, the benzylated compound **1d** catalyses also quite well with 7.2 turn-overs. Here the steric pressure should be a problem, but by introducing an aromatic ring in the second coordination shell there might be a predominating electronic effect on the catalytic cycle. As a result, this ligand increases the stability of the complex, which leads to more turn-overs (27.6) than **1a** after a second and third addition of two equivalents photosensitiser each after 48 and 70 hours. Despite that, the most important insight of the platinum series is the actual non-activity of the control sample without proton relay. The very small detected amount of hydrogen of the control sample may be credited with the photosensitiser itself.

Table 1 Hydrogen production of the platinum series, WRC/PS = 1 at the beginning, after 24 h and 48 h addition of two equivalents of PS each, irradiation with 150 W Hg medium pressure lamp, maximal relative standard deviation 1.5%

Compound	TON	TON	TON
2a	10.7	12.6	14.4
2b	1.8	3.4	4.8
2c	2.1	3.4	4.5
2d	7.2	22.8	27.6
Control	0.4	1.1	2.1
PS/WRC	1	3	5
Irradiation time	t = 24 h	t = 48 h	t = 70 h

Structural analysis on catalyst complexes containing at least one PNP ligand by single crystal X-ray diffractometry

The molecule structures of $[Pd(PNP\text{-}C1\text{-}Me)_2](BF_4)_2$ **1a** , $[PdCl_2(PNP\text{-}C1\text{-}Me)]$ **3a**, $[NiCl_2(PNP\text{-}C1\text{-}Me)]$ **5a**, $[NiCl_2(PNP\text{-}C1\text{-}iPr)]$ **5c** and $[PdCl(PNP\text{-}C2\text{-}Me)](PF_6)$ **9** are shown below. All structures show the precatalyst with the metal centre in the oxidation state of +II. Whether the metal is palladium or nickel, the complex is a heteroleptic chlorido or a homoleptic one, the PNP ligand is substituted with a methyl or a sterically more challenging *iso*-propyl group and whether the ligand backbone is short with PNP-C1 or long with PNP-C2 each and every precatalyst shows a square planar structure concerning metal centre and coordination partners.

CCDC-1874808 (for **1a**), -1874809 (for **3a**), -1874810 (for **5a**), -1874811 (for **5c**), and -1874812 (for **9**) contain the supplementary crystallographic data for this paper. These data can be obtained free of charge from The Cambridge Crystallographic Data Centre via www.ccdc.cam.ac.uk/data_request/cif

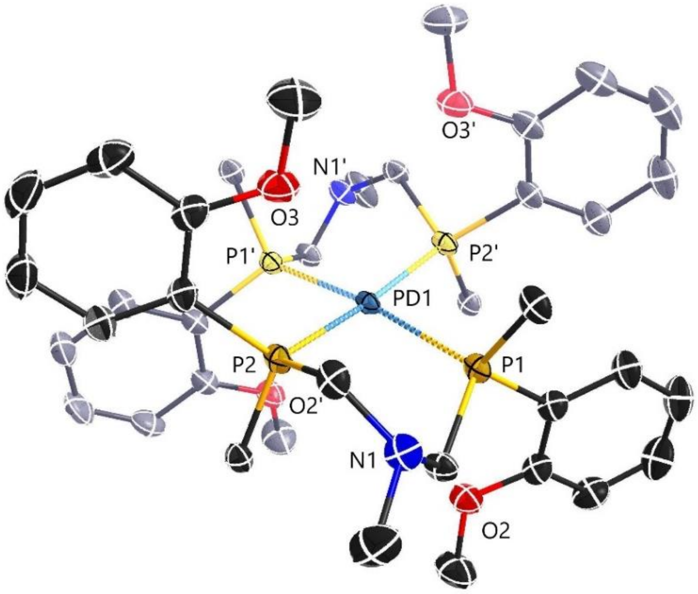

*Figure 2: ORTEP representations by XRD analysis of $[Pd(II)(PNP\text{-}C1\text{-}methyl)_2](BF_4)_2$ **1a**, anions, hydrogens and solvent molecules omitted for clarity. Selected bond lengths and intramolecular distances [Å]: P1-PD1 2.3920(8), P2-PD1 2.3782(7), N1 PD1 4.037(2), O2 PD1 3.915(11), O3 PD1 3.726(11).*

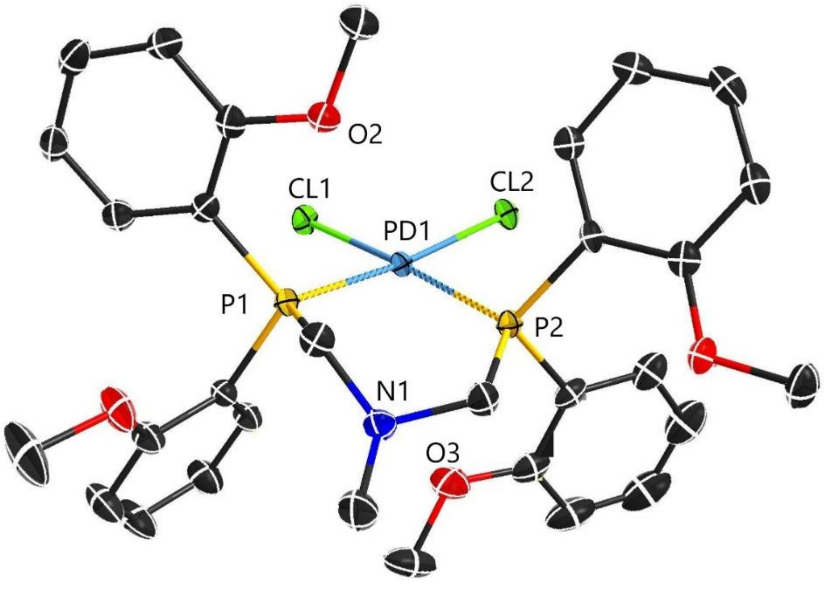

*Figure 3: ORTEP representations by XRD analysis of $[Pd(II)Cl_2(PNP\text{-}C1\text{-}methyl)]$ **3a**, anions, hydrogens and solvent molecules omitted for clarity. Selected bond lengths and intramolecular distances [Å]: CL1-PD1 2.3438(5), CL2-PD1 2.3762(5), P1-PD1 2.2403(5), P2-PD1 2.2602(5), N1 PD1 3.662(3), O2 PD1 3.405 (8), O3 PD1 3.498(13).*

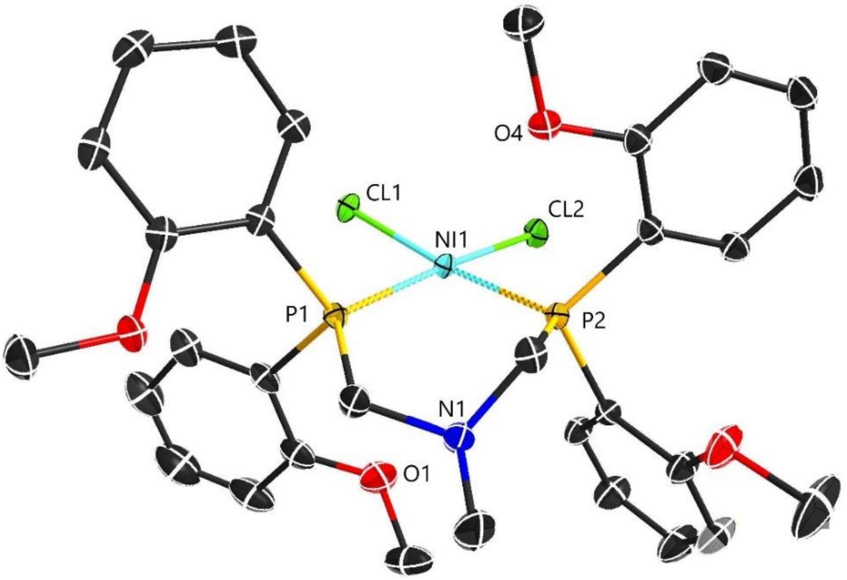

Figure 4: ORTEP representations by XRD analysis of [Ni(II)Cl_2(PNP-C1-methyl)] ***5a****, anions, hydrogens and solvent molecules omitted for clarity. Selected bond lengths and intramolecular distances [Å]: CL1-NI1 2.2242(3), CL2-NI1 2.1964(3), P1-NI1 2.1878(3), P2-NI1 2.1645(3), N1 NI1 3.647(3), O1 NI1 3.437(12), O4 NI1 3.377(7).*

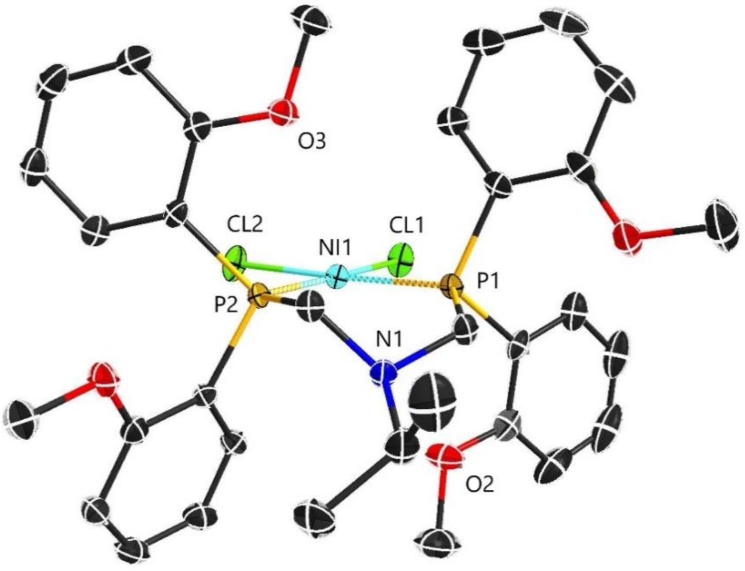

Figure 5: ORTEP representations by XRD analysis of [Ni(II)Cl_2(PNP-C1-iso-propyl)] ***5c****, anions, hydrogens and solvent molecules omitted for clarity. Selected bond lengths and intramolecular distances [Å]: CL1-NI1 2.2090(4), CL2-NI1 2.1995(4), P1-NI1 2.1765(4), P2-NI1 2.1711(4), N1 NI1 3.598(2), O2 NI1 3.588(15), O3 NI1 3.617(5).*

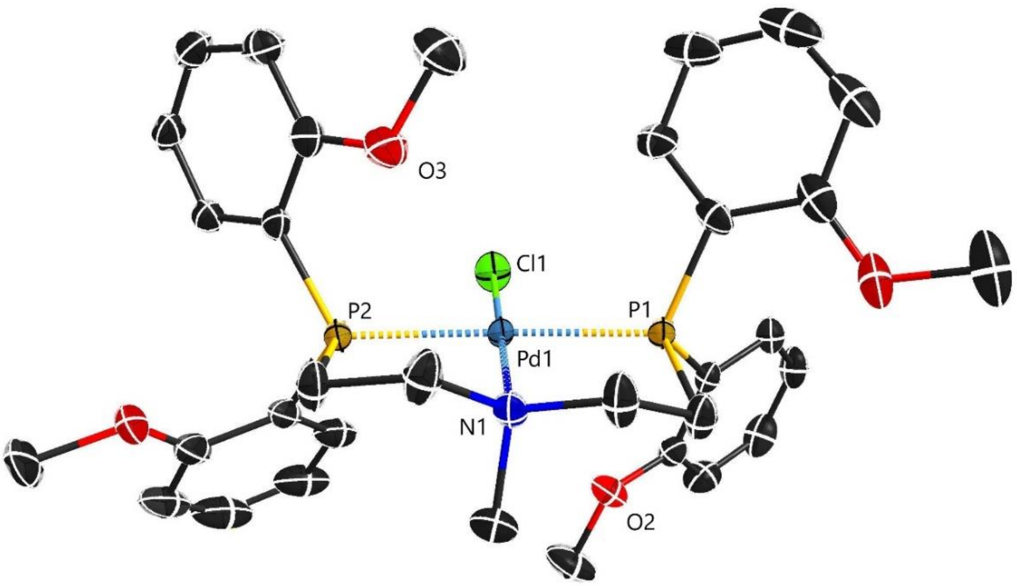

Figure 6: ORTEP representations by XRD analysis of [Pd(II)Cl(PNP-C2-methyl)](PF$_6$) ***9****, anions, hydrogens and solvent molecules omitted for clarity. Selected bond lengths and intramolecular distances [Å]: Cl1-Pd1 2.3036(8), P1-Pd1 2.2962(8), P2-Pd1 2.3055(8), N1-Pd1 2.086(3), O2 Pd1 3.241(19), O3 Pd1 3.272(16).*

Proposal of catalytic cycle of [Ni(II)(CH_3CN)$_2$(PNP-C1)]$^{2+}$

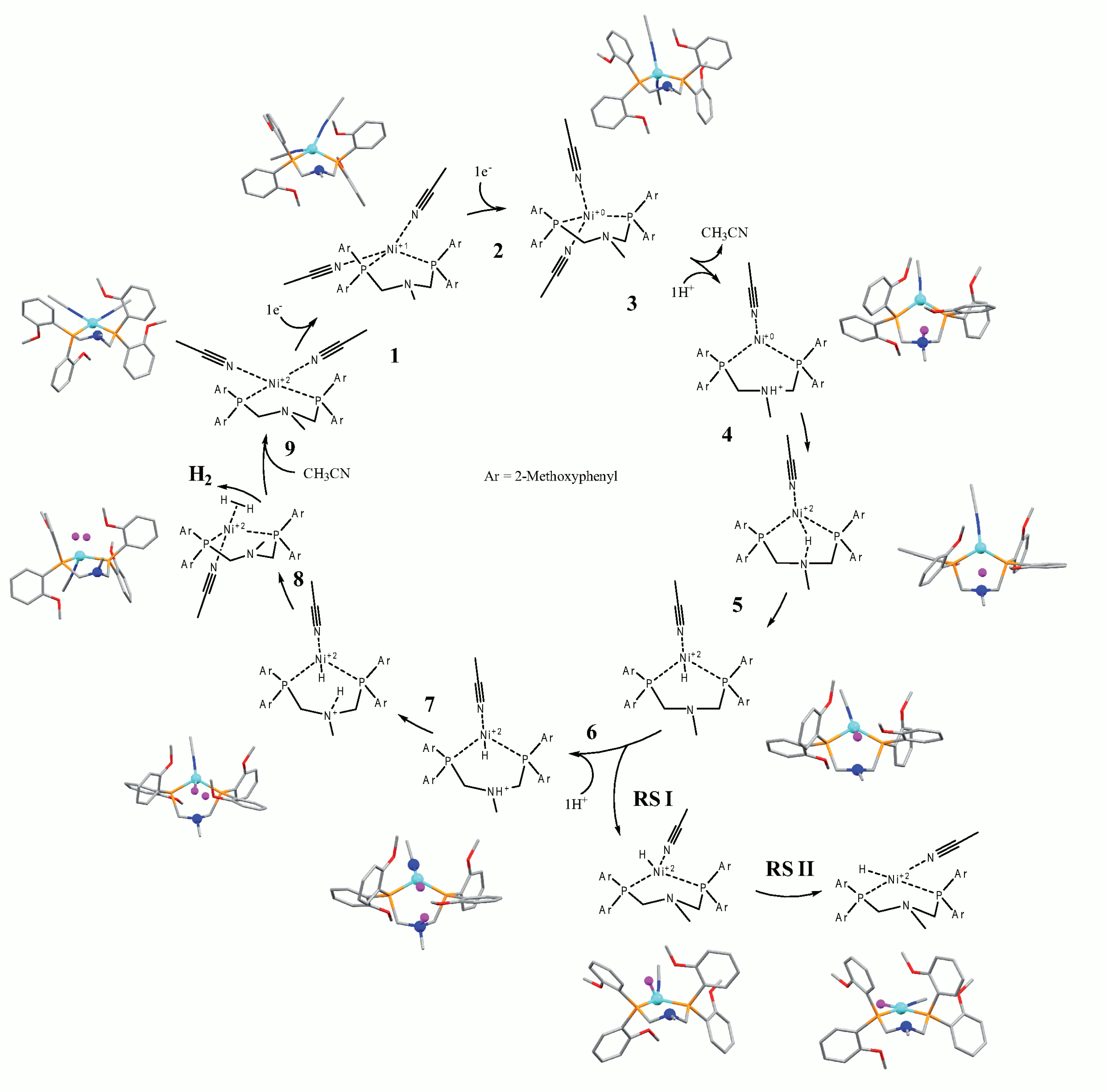

Figure 7: Dissociative catalytic cycle of [Ni(II)(CH_3CN)$_2$(PNP-C1-Me)](PF_6)$_2$ ***8****, drawn as structural formula on the inside, surrounded by the respective structure obtained from DFT calculations (wireframe-style for all atoms except of the metal centre, pendant amine and reacting hydrogens, shown as 'ball and stick'; carbon in grey, hydrogen in purple, nitrogen in dark blue, oxygen in red, phosphorus in orange, nickel in light blue)*

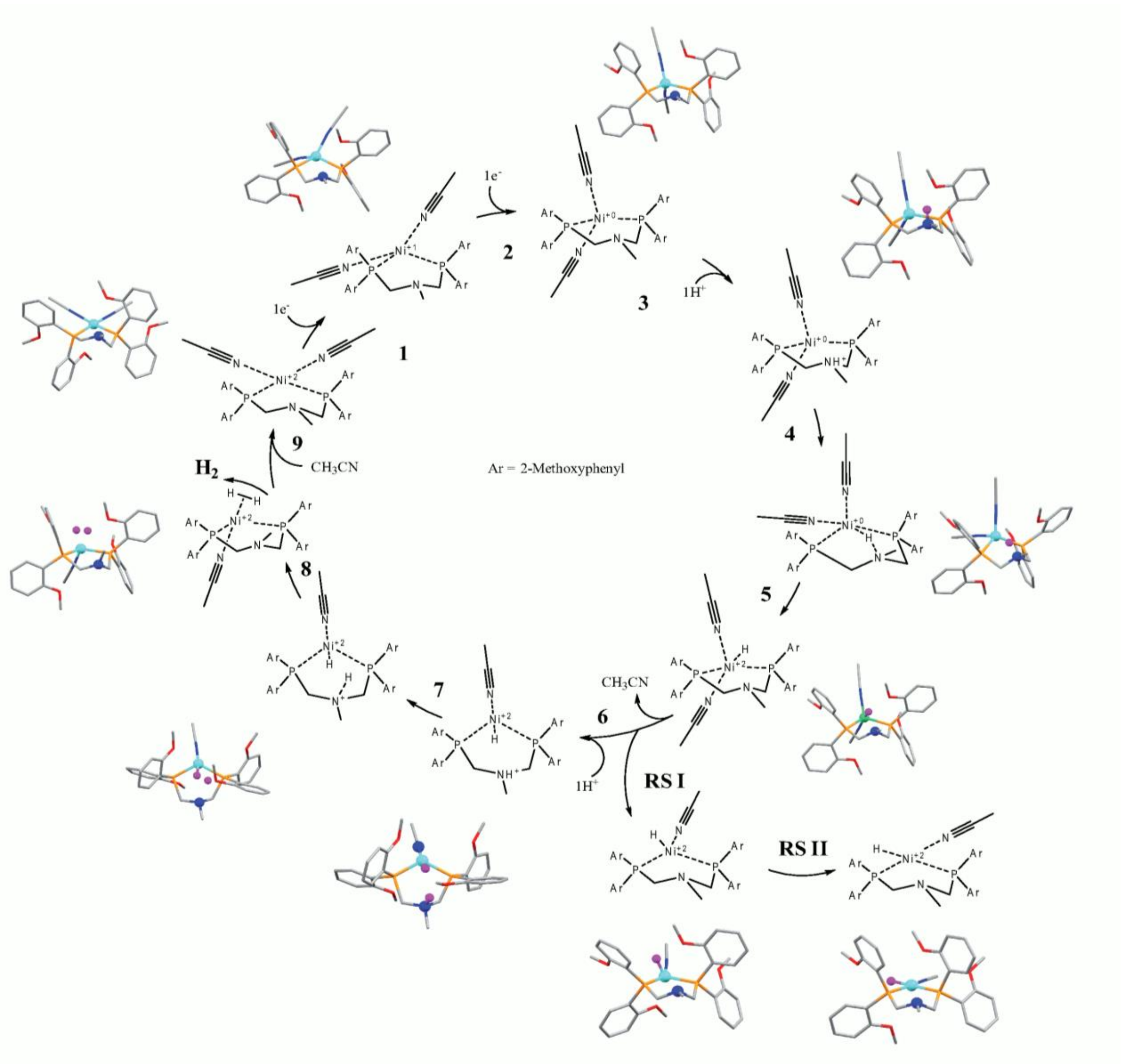

Figure 8: Associative catalytic cycle of $[Ni(II)(CH_3CN)_2(PNP\text{-}C1\text{-}Me)](PF_6)_2$ ***8****, drawn as structural formula on the inside, surrounded by the respective structure obtained from DFT calculations (wireframe-style for all atoms except of the metal centre, pendant amine and reacting hydrogens, shown as 'ball and stick'; carbon in grey, hydrogen in purple, nitrogen in dark blue, oxygen in red, phosphorus in orange, nickel in light blue)*

Table 2: Energy levels of [Ni(II)(ACN)$_2$PNP-C1-Me]$^{2+}$ in gas phase (combined energies of dissociative and associatice (orange) cycle)

Cat.-step	log file	E /Hartree	E /kJmol^{-1}	Delta E /kJmol^{-1}	Comment
1	1_Ni2_2acn.xyz	-4.014,213198900	-10539308,73	3661,60	Precatalyst
2	2_Ni1_low_2acn.xyz	-4.014,495942230	-10540051,07	2919,26	Nickel in Ox +1
3	3_Ni0_2acn.xyz	-4.014,607596200	-10540344,21	2626,11	Activated Catalyst in OX 0
4a	4a_proton_2acn.xyz	-4.015,304111210	-10542172,91	797,42	Protonated with 2 ACN
4b	4b_proton_1acn.xyz	-3.882,534688810	-10193587,06	833,61	Protonated with 1 ACN
5a	5a_proton_TS_2acn.xyz	-4.015,295334850	-10542149,87	820,46	TS 1st proton with 2 ACN
5b	5b_proton_TS_1acn.xyz	-3.882,526057250	-10193564,40	856,27	TS 1st proton with 1 ACN
6a	6a_hydride_2acn.xyz	-4.015,303849380	-10542172,23	798,10	Nickelhydride with 2 ACN
6b	6b_hydride_1acn.xyz	-3.882,535007670	-10193587,90	832,77	Nickelhydride with 1 ACN
6c	6c_protonswap_TS_1acn.xyz	-3.882,520402720	-10193549,55	871,12	TS to resting state
6d	6d_protonswap_1acn.xyz	-3.882,545691190	-10193615,95	804,72	Resting state
7	7_2proton_1acn.xyz	-3.882,852193120	-10194420,67	0,00	2nd Protonation with 1 ACN
8	8_2proton_TS_1acn.xyz	-3.882,803212830	-10194292,07	128,60	TS 2nd proton with 1 ACN
9	9_h2_release.xyz	-3.882,820746890	-10194338,11	82,56	H_2 Release

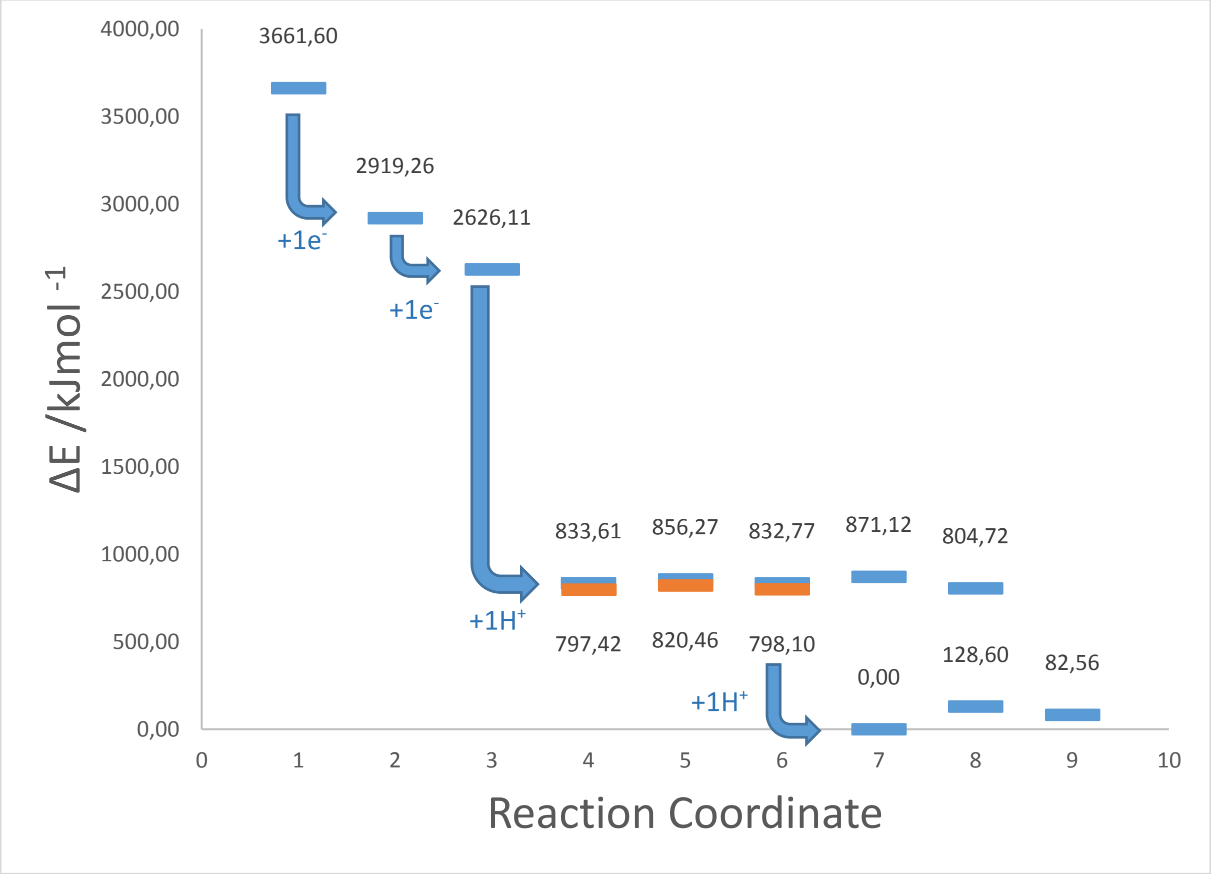

Figure 9: Energy diagram of all steps within the catalytic cycle of [Ni(II)(ACN)$_2$PNP-C1-Me]$^{2+}$ in gas phase (combined energies of dissociative and associative (orange) cycle)

Table 3: Energy levels of [Ni(II)(ACN)$_2$PNP-C1-Me]$^{2+}$ in solvent environment (combined energies of dissociative and associatice (orange) cycle)

Cat.-step	log file	E /Hartree	E /kJmol^{-1}	Delta E /kJmol^{-1}	Comment
1	1_Ni2_2acn.xyz	-4.014,627599750	-10540396,73	3060,13	Precatalyst
2	2_Ni1_low_2acn.xyz	-4.014,773199850	-10540779,01	2677,85	Nickel in Ox +1
3	3_Ni0_2acn.xyz	-4.014,898858570	-10541108,92	2347,94	Activated Catalyst in OX 0
4a	4a_proton_2acn.xyz	-4.015,369867250	-10542345,56	1111,31	Protonated with 2 ACN
4b	4b_proton_1acn.xyz	-3.882,598196950	-10193753,80	1153,40	Protonated with 1 ACN
5a	5a_proton_TS_2acn.xyz	-4.015,3547815500	-10542305,95	1150,91	TS 1st proton with 2 ACN
5b	5b_proton_TS_1acn.xyz	-3.882,5828426100	-10193713,49	1193,71	TS 1st proton with 1 ACN
6a	6a_hydride_2acn.xyz	-4.015,361434090	-10542323,41	1133,45	Nickelhydride with 2 ACN
6b	6b_hydride_1acn.xyz	-3.882,591841300	-10193737,11	1170,09	Nickelhydride with 1 ACN
6c	6c_protonswap_TS_1acn.xyz	-3.882,5774856900	-10193699,42	1207,78	TS to resting state
6d	6d_protonswap_1acn.xyz	-3.882,599928490	-10193758,35	1148,85	Resting state
7	7_2proton_1acn.xyz	-3.883,037503580	-10194907,20	0,00	2nd Protonation with 1 ACN
8	8_2proton_TS_1acn.xyz	-3.882,9839005500	-10194766,46	140,73	TS 2nd proton with 1 ACN
9	9_h2_release.xyz	-3.883,000284900	-10194809,48	97,72	H_2 Release

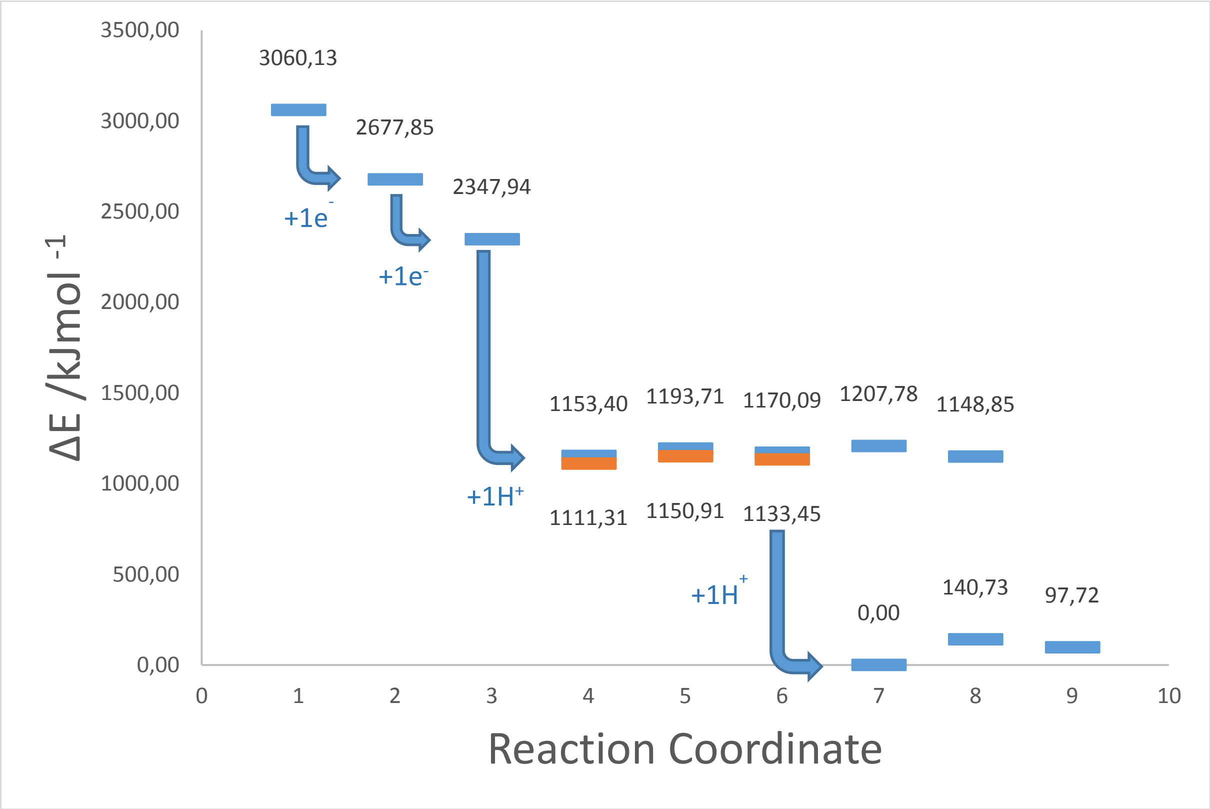

Figure 10: Energy diagram of all steps within the catalytic cycle of [Ni(II)(ACN)$_2$PNP-C1-Me]$^{2+}$ in solvent environment (combined energies of dissociative and associative (orange) cycle)

Proposal of catalytic cycle of [Ni(II)Cl(PNP-C2)]$^+$

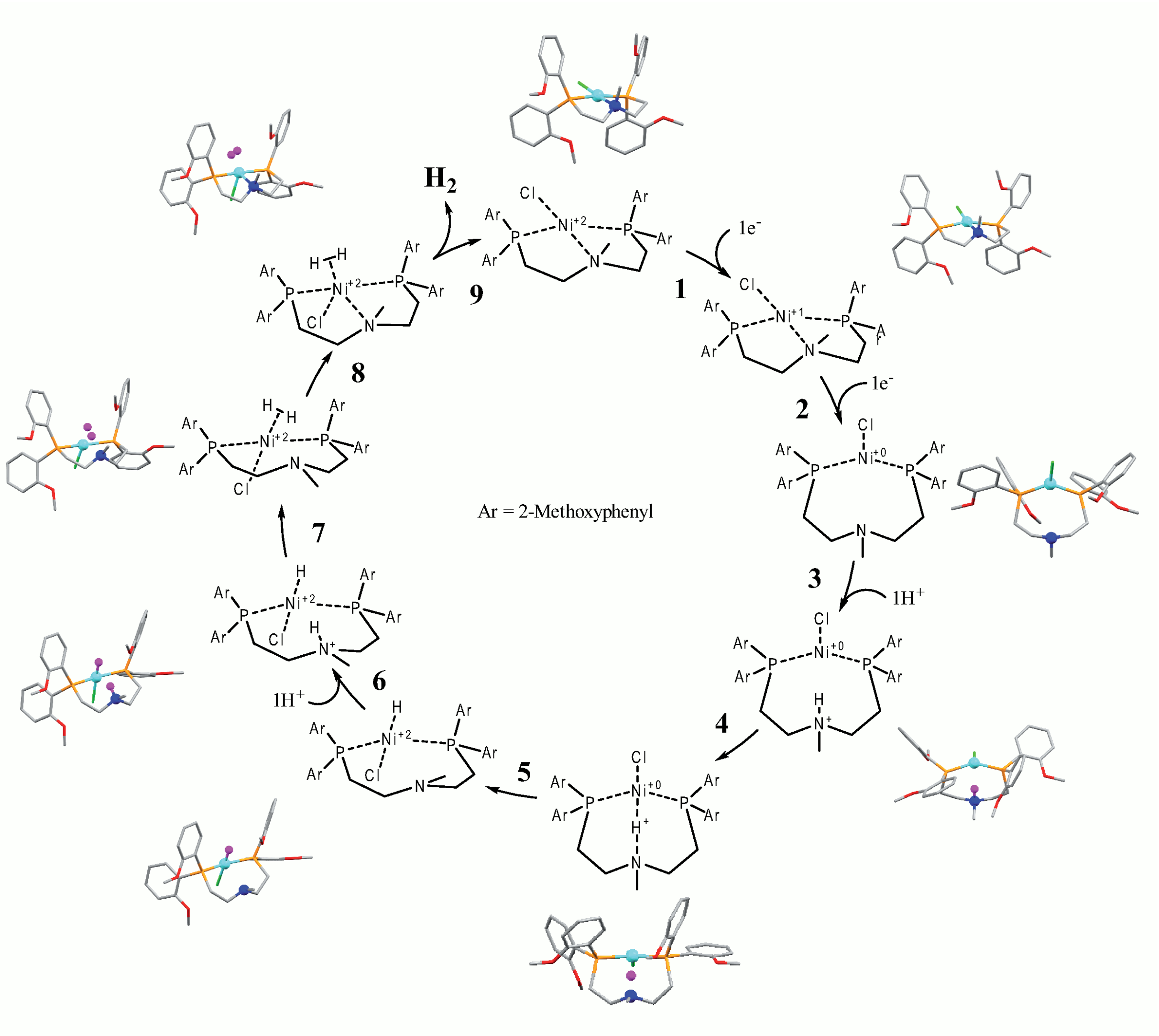

Figure 11: Catalytic cycle of [Ni(II)Cl(PNP-C2-Me)]$^+$, drawn as structural formula on the inside, surrounded by the respective structure obtained from DFT calculations (wireframe-style for all atoms except of the metal centre, pendant amine and reacting hydrogens, shown as 'ball and stick'; carbon in grey, hydrogen in purple, nitrogen in dark blue, oxygen in red, phosphorus in orange, nickel in light blue)

Table 4: Energy levels of [Ni(II)Cl(PNP-C2-Me)]⁺ in gas phase

Cat.-step	log file	E /Hartree	E /kJmol^{-1}	Delta E /kJmol^{-1}	Comment
1	1_Ni2	-4.287,8418634800	-11257720,24	3022,87	Precatalyst
2	2_Ni1_low.xyz	-4.287,9921108800	-11258114,71	2628,39	Nickel in Ox +1
3	3_Ni0	-4.287,991806320	-11258113,91	2629,19	Activated Catalyst
4	4_Ni0_protonated	-4.288,531196990	-11259530,08	1213,02	1st Protonation
5	5_Ni0_TS1	-4.288,530362940	-11259527,89	1215,21	TS 1st proton
6	6_Ni2_hydride	-4.288,566636730	-11259623,13	1119,98	Nickelhydride
7	7_Ni2_2nd_proton	-4.288,993214010	-11260743,11	0,00	2nd Protonation
8	8_Ni2_TS2	-4.288,970166310	-11260682,59	60,51	TS 2nd proton
9	9_Ni2_H2_release	-4.288,977056430	-11260700,68	42,42	H_2 release

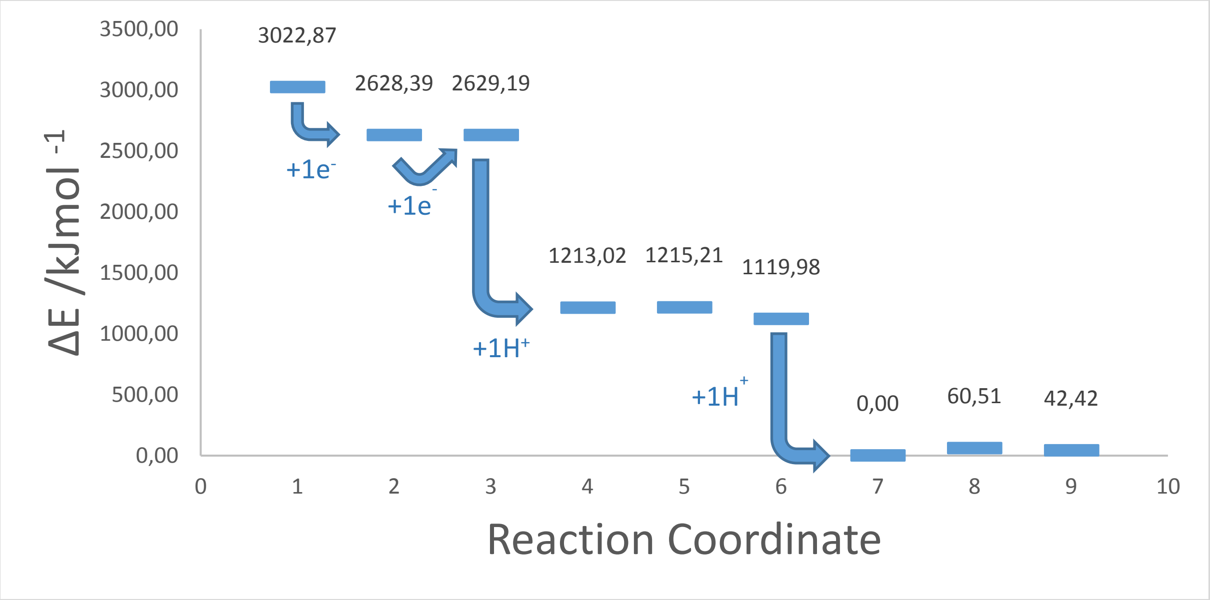

Figure 12: Energy diagram of [Ni(II)Cl(PNP-C2-Me)]⁺ in gas phase

Table 5: Energy levels of [Ni(II)Cl(PNP-C2-Me)]$^+$ in solvent environment

Cat.-step	log file	E /Hartree	E /kJmol^{-1}	Delta E /kJmol^{-1}	Comment
1	1_Ni2	-4.288,1617622600	-11258560,13	3051,25	Precatalyst
2	2_Ni1_low.xyz	-4.288,2796089600	-11258869,54	2741,84	Nickel in Ox +1
3	3_Ni0	-4.288,3771346400	-11259125,59	2485,79	Activated Catalyst
4	4_Ni0_protonated	-4.288,8623528700	-11260399,53	1211,85	1st Protonation
5	5_Ni0_TS1	-4.288,8619632000	-11260398,51	1212,87	TS 1st proton
6	6_Ni2_hydride	-4.288,8585830900	-11260389,63	1221,75	Nickelhydride
7	7_Ni2_2nd_proton	-4.289,3239225900	-11261611,38	0,00	2nd Protonation
8	8_Ni2_TS2	-4.289,2748457400	-11261482,53	128,85	TS 2nd proton
9	9_Ni2_H2_release	-4.289,3064222300	-11261565,43	45,95	H_2 release

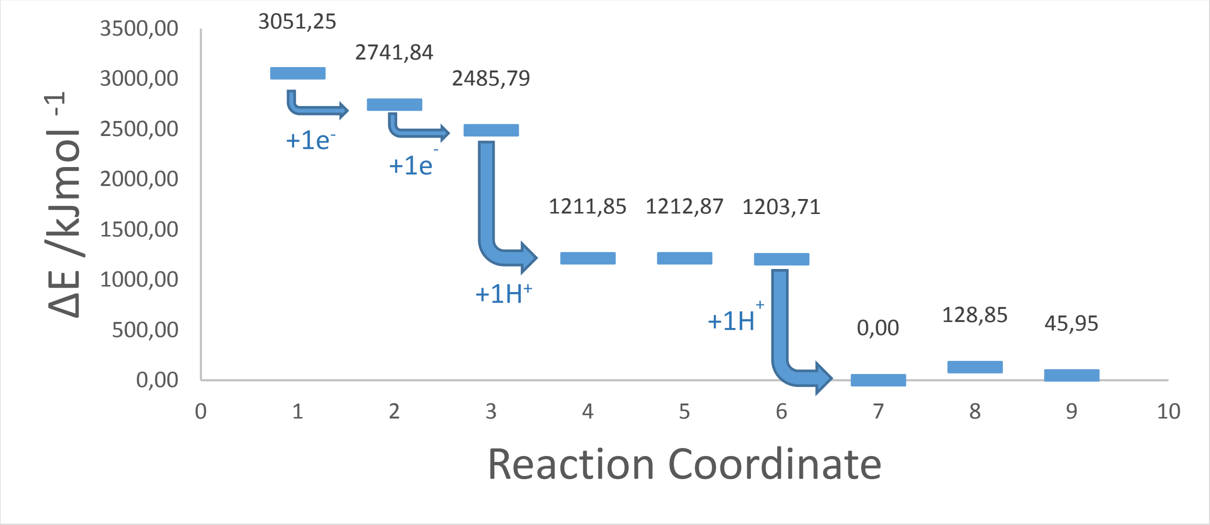

Figure 13: Energy diagram of [Ni(II)Cl(PNP-C2-Me)]$^+$ in solvent environment

Experimental section

Synthesis

The syntheses of the PNP-C1 ligands, their metal complexes $[M(II)(PNP\text{-}C1)_2](BF_4)_2$ and $[M(II)Cl_2(PNP\text{-}C1)_2]$ are all very similar, and the procedures and characterization data are given for representative examples only. Below one can find procedure details and data for PNP-C1-methyl, PNP-C2-methyl, $[Pd(II)(PNP\text{-}C1\text{-}methyl)_2](BF_4)_2$ **1a,** $[Ni(II)Cl_2(PNP\text{-}C1\text{-}methyl)]$ **5a**, $[Ni(II)(CH_3CN)_2(PNP\text{-}C1\text{-}methyl)](BF_4)_2$ **8** and $[Pd(II)Cl(PNP\text{-}C2\text{-}methyl)_2](PF_6)$ **9**. Spectroscopic characterization data for the remaining ligands and complexes are published elsewhere[1]. The control ligand PCCCP without proton relay was prepared as discribed in literature[2] and its complexes $[Pd(II)(PCCCP)_2](PF_6)_2$ and $[Pt(II)(PCCCP)_2](PF_6)_2$ are prepared analogously to $[M(II)(PNP\text{-}C1)_2](PF_6)_2$.

***N,N*-Bis-[(di-(2-methoxyphenyl)phosphino)methyl]-*N*-methylamine (PNP-C1-Me).** Methylamine hydrochloride (43.0 mg, 0.63 mmol) is neutralised by stirring with potassium *tert*-butoxide (70.7 mg, 0.63 mmol) in 10 mL THF/MeOH (1:1) for five minutes. The resulting mixture is added to a solution of di-(2methoxyphenyl)phosphane (311.2 mg, 1.26 mmol) and paraformaldehyde (38.2 mg, 1.26 mmol) in 10 mL THF/MeOH (1:1). The combined solution is stirred at ambient temperature for 17 hours. Due to the low boiling points of methylamine and formaldehyde a ^{31}P-NMR reaction control is quite reasonable. The solvent is removed and the crude product is extracted in toluene and water. The organic phase is concentrated and the product is precipitated three times with 20 mL of hexane. The white powder is filtrated and dried under *vacuum* (268.8 mg, 0.491 mmol, Yield: 78%). Crystals can be obtained by inverse gasphase diffusion in toluene and a pentane/hexane mixture (1:1, v/v). Mp: 135 °C. Calculated for $C_{31}H_{35}NO_4P_2$ (547.56): C, 68.00, H, 6.44, N, 2.56; Found: C, 67.91, H, 6.53, N, 2.53%. $^{31}P\{^1H\}$-NMR (121.497 MHz, Toluene): δ (ppm) = -42,729 (s, P). ^1H-NMR (300.13 MHz, CD_2Cl_2): δ (ppm) = 7.294 (m, 4H, H^{Ar}), 7.163 (m, 4H, H^{Ar}), 6.855 (m, 8H, H^{Ar}), 3.743 (s, 12H, H^{MeO}), 3.438 (4H, s, $CH_2^{N;P}$), 2.635 (s, 3H, CH_3). ^{31}C-NMR (75.476 MHz, CD_2Cl_2): δ (ppm) = 161.638 (s, 4C, C^{Ar}), 133.823 (s, 4C, C^{Ar}), 130.440 (s, 4C, C^{Ar}), 125.360 (s, 4C, C^{Ar}), 121.319 (s, 4C, C^{Ar}), 110.915 (s, 4C, C^{Ar}), 58.002 (s, 2C, $CH_2^{N,P}$), 56.003 (s, 4C, MeO), 30.266 (s, 1C, CH_3). MALDI-MS (TOF-TOF): Observed $C_{31}H_{34}NO_4P_2$ (deprotonated) at m/z = 546.2, calculated 546.5; observed $C_{31}H_{36}NO_4P_2$ (protonated) at m/z = 548.3, calculated 548.5.

***N,N*-Bis-[(di-(2-methoxyphenyl)phosphino)ethyl]-*N*-methylamine (PNP-C2-Me).** Di-(2-methoxyphenyl)phosphane (400.5 mg, 1.62 mmol) is dissolved in 20 mL DMSO with 2-3 g of molecular sieve (4 Å). To activate the phosphane $CsOH·H_2O$ (816.2 mg, 4.86 mmol) is added resulting in a colour change from colourless to dark red. A second solution of 20 mL DMSO is prepared with 2-3 g of molecular sieve. *N,N*-Bis-(2 chloroethyl)-*N*-methylamine stabilised with hydrochloric acid, HN2·HCl, (155.9 mg, 0.81 mmol) is added and neutralised a stoichiometric amount of $CsOH·H_2O$. This mixture is filtrated to remove the molecular sieve and added to the activated phosphane by a dropping funnel within 2 h. Then combined solution is stirred at ambient temperature for 17 h. The resulting yellow mixture is distilled to remove DMSO. With 30 mL of 1,2-dichlorethane the crude product is dissolved and filtrated to remove molecular sieve. The solvent is removed and the residue dissolved in 25 ml of toluene. The organic phase is extracted three times with 20 mL of deionised water and concentrated to obtain a dark yellow oil (303.6 mg, 0.527 mmol, yield: 65%). Calculated for $C_{33}H_{39}NO_4P_2$ (575.61): C, 68.86, H, 6.83, N, 2.43; Found: C, 68.79, H, 6.93, N, 2.37%. $^{31}P\{^1H\}$-NMR (121.497 MHz, CD_2Cl_2): δ (ppm) = -36.802 (s, 2P). ^1H-NMR (300.13 MHz, CD_2Cl_2): δ (ppm) = 7.440-7.261 (m, 10H, H^{Ar}), 7.045-6.935 (m, 6H, H^{Ar}), 3.817 (s, 12H, H^{MeO}), 2.685 (dd, $^3J_{H\text{-}H}$ = 69.03 Hz, $^2J_{P\text{-}H}$ = 7.803 Hz, 4H, PCH_2), 2.457 (s, 3H, CH_3), 2.413 (pseudo t, $^3J_{H\text{-}H}$ = 12.31 Hz (?), 4H, NCH_2). ^{13}C-NMR (75.476 MHz, CD_2Cl_2): δ (ppm) = 162.011 (s, 4C, C^{Ar}), 133.281 (d, 4C, C^{Ar}), 130.384 (s, 4C, C^{Ar}), 125.804, 128.714. 129,508 (3s, 4C, C^{Ar}), 121.359 (s, 4C, C^{Ar}), 110.922 (s, 6C, C^{Ar}), 55.903 (s, 4C, MeO), 54.805 (s, 2C, NCH_2), 41.978 (s, 1C, CH_3), 21.763 (s, 2C, PCH_2). MALDI-MS (TOF-TOF): Observed $C_{33}H_{38}NO_4P_2$ (deprotonated) at m/z = 574.4, calculated 574.6;

$[Pd(II)(PNP\text{-}C1\text{-}methyl)_2](BF_4)_2$ 1a. Tetrakis-(acetonitrile)-palladium(II)-tetrafluoroborate (10.8 mg, 0.0243 mmol) is dissolved in 20 mL 1,2-dichlorethane. To the colourless solution is added PNP-C1-Me (26.6 mg, 0.0486 mmol) by a slightly colour change to yellow. This solution is stirred for 17 hours at ambient temperature. Afterwards the solvent is changed to toluene and the solution is filtrated. The solid is dissolved in dichlormethane and precipitated again three times with 20 ml hexane. The yellow powder is dried under vacuum (24.1 mg, 0.0175 mmol, Yield: 72.1 %). Crystals can be obtained by inverse gasphase diffusion in dichloromethane and hexane. Mp: 147 °C. Calculated for $C_{62}H_{70}B_2F_8N_2O_8P_4Pd·3.56CH_2Cl_2·0.38H_2O$ (1684.33): C, 46.75, H, 4.66, N, 1.66; Found: C, 46.67, H, 4.73, N, 1.61%. $^{31}P\{^1H\}$-NMR (121.497 MHz, 1,2-CH_2Cl_2): δ (ppm) = 10.873 (s, 2P). ^1H-NMR (300.13 MHz, CD_2Cl_2): δ (ppm) = 7,94 (m, 4H, H^{Ar}), 7.53 (m, 4H, H^{Ar}), 7.01 (m, 8H, H^{Ar}), 3.69 (s, 12H, H^{MeO}), 3.57 (4H, s, $CH_2^{N,P}$), 2.18 (s, 3H, CH_3). ^{13}C-NMR (75.476 MHz, CD_2Cl_2): δ (ppm) = 161.505 (s, 4C, C^{Ar}), 135.764 (s, 4C, C^{Ar}), 130.280 (s, 4C, C^{Ar}), 125.360 (s, 4C, C^{Ar}), 127.817 (s, 4C, C^{Ar}), 112.050 (s, 4C, C^{Ar}), 57.952 (s, 2C, $CH_2^{N,P}$), 56.320 (s, 4C, MeO), 32.254 (s, 1C, CH_3). MALDI-MS (TOF-TOF): Observed $C_{31}H_{34}NO_4P_2Pd$ (without two counterions, one ligand and one hydrogen atom) at m/z = 653.1, calculated 653.0.

$[Ni(II)Cl_2(PNP\text{-}C1\text{-}methyl)_2]$ 5a. PNP-C1-Me (38.8 mg, 0.0710 mmol) is dissolved in 20 mL of 1,2-dichlorethane. To this solution $Ni(II)Cl_2·(H_2O)_6$ (16.9 mg, 0.0710 mmol) was added to turn the colourless solution slightly orange. The salt is dissolving very slowly, so the reaction mixture is stirred at ambient temperature for 17 h until a strong red solution is obtained. The solvent is removed. The resulting red powder is crystallised in ACN/diethyl ether. The product are red crystals. (40.7 mg, 0.0600 mmol, Yield: 84.5 %). Crystals can be obtained by inverse gasphase diffusion in acetonitrile and diethylether. Mp: 180 °C. Calculated for $C_{31}H_{35}Cl_2NNiO_4P_2·C_2H_3N$ (718.18): C, 55.19, H, 5.33, N, 3.90; Found: C, 55.11, H, 5.41, N, 3.81%. $^{31}P\{^1H\}$-

NMR (121.497 MHz, 1,2-CH_2Cl_2): δ (ppm) = 3.645 (s, 2P). ^{1}H-NMR (300.13 MHz, CD_2Cl_2): δ (ppm) = 8.318 (m, 4H, H^{Ar}), 7.510 (m, 4H, H^{Ar}), 7.054 (m, 8H, H^{Ar}), 3.780 (s, 12H, H^{MeO}), 2.143 (s, 4H, $CH_2^{N,P}$), 1.517 (3H, s, CH_3). ^{13}C-NMR (75.476 MHz, $CDCl_3$): δ (ppm) = 161.519 (s, 4C, C^{Ar}), 140.946 (s, 4C, C^{Ar}), 133.400 (s, 4C, C^{Ar}), 129.479 (s, 4C, C^{Ar}), 120.084 (s, 4C, C^{Ar}), 111.501 (s, 4C, C^{Ar}), 56.160 (s, 4C, MeO), 55.789 (s, 2C, $CH_2^{N,P}$), 28.667 (s, 1C, CH_3). MALDI-MS (TOF-TOF): Observed $C_{31}H_{34}Cl_2NO_4P_2Ni$ (deprotonated) at m/z = 676.2, calculated 676.2; observed $C_{31}H_{34}Cl_1NO_4P_2Ni$ (dechlorinated) at m/z = 641.7, calculated 641.3.

[Ni(II)(CH_3CN)$_2$(PNP-C1-methyl)](BF_4)$_2$ 8. PNP-C1-Me (70.3 mg, 0,1284 mmol) is dissolved in 20 mL of acetonitrile. To this solution Ni(II)(BF_4)$_2$·(H_2O)$_6$ (43.70 mg, 0,1284 mmol) was added. Then there is a colour change to red. The reaction mixture is stirred at ambient temperature for 17 h until a strong red solution is obtained. The solvent is removed. Next the red powder is dissolved in dichloromethane and precipitated with hexane three times. The product is a red powder. (70.64 mg, 0,08195 mmol, Yield: 64 %). Mp: 136 °C. Calculated for $C_{35}H_{41}B_2F_8N_3NiO_4P_2$ (861.95): C, 48.77, H, 4.79, N, 4.88; Found: C, 48.73, H, 4.83, N, 4.85%. ^{31}P{^{1}H}-NMR (121.497 MHz, CD_2Cl_2): δ (ppm) = -13.486 (s, 2P). ^{1}H-NMR (300.13 MHz, CD_2Cl_2): δ (ppm) = 7.547 (m, 4H, H^{Ar}), 7.293 (m, 2H, H^{Ar}), 7.061 (m, 4H, H^{Ar}), 6.853 (m, 6H, H^{Ar}), 4.159 (s, 12H, H^{MeO}), 3.473 (s, 4H, $CH_2^{N,P}$), 2.563 (3H, s, CH_3), 1.808 (6H, s, $NCCH_3$). ^{31}C-NMR (75.476 MHz, CD_2Cl_2): δ (ppm) = 160.999 (s, 4C, C^{Ar}), 135.680 (s, 4C, C^{Ar}), 133.153 (s, 4C, C^{Ar}), 122.370 (s, 4C, C^{Ar}), 121.517 (s, 4C, C^{Ar}), 111.955 (s, 4C, C^{Ar}), 110.625 (s, 2C, $NCCH_3$), 57.085 (s, 2C, $CH_2^{N,P}$), 56.295 (s, 4C, MeO), 49.813 (s, 1C, CH_3), 3.021 (s, 2C, $NCCH_3$). MALDI-MS (TOF-TOF): Observed $C_{35}H_{41}B_2F_7N_3NiO_4P_2$ (without one fluorine) at m/z = 843.2, calculated 843.0.

[Pd(II)Cl(PNP-C2-methyl)](PF_6) 9. [$PdCl_2$(COD)] (33.61 mg, 0.118 mmol) is dissolved in 20 mL acetonitrile and PNP-C2-Me (67.92 mg, 0.118 mmol) and Na(PF_6) (19.82 mg, 0.118 mmol) are added. After stirring for 12 hours the solution is concentrated and precipitated with diethyl ether. The yellow powder can be crystallised with 1,2-dichlorethane/(hexane:pentane) (1:1:1). The product are yellow crystals. (93.45 mg, 0.108 mmol, Yield: 91.5%). Crystals can be obtained by inverse gasphase diffusion in 1,2-dichloroethane and diethylether. Mp: 163 °C. Calculated for $C_{33}H_{39}ClF_6NO_4P_3Pd\cdot C_2H_4Cl_2\cdot 0.4H_2O$ (968.62): C, 43.40, H, 4.56, N, 1.45; Found: C, 43.33, H, 4.66, N, 1.39%. ^{31}P{^{1}H}-NMR (121.497 MHz, CD_3CN): δ (ppm) = 34.445 (s, 2P). ^{1}H-NMR (300.13 MHz, CD_3CN): δ (ppm) = 7.682 (m, 4H, H^{Ar}), 7.553 (m, 4H, H^{Ar}), 7.243 (m, 4H, H^{Ar}), 7.079 (m, 4H, H^{Ar}), 3.951 (s, 12H, H^{MeO}), 3.083 (m, 4H, PCH_2), 2.802 (s, 3H, CH_3), 1.940 (q, $^3J_{H-H}$ = 9.904 Hz, 4H, NCH_2). ^{13}C-NMR (75.476 MHz, CD_3CN): δ (ppm) = 162.397 (s, 4C, C^{Ar}), 132.784 (s, 4C, C^{Ar}), 129.947 (s, 4C, C^{Ar}), 122.424 (s, 4C, C^{Ar}), 118.688 (s, 4C, C^{Ar}), 112.377 (s, 6C, C^{Ar}), 57.330 (s, 4C, MeO), 56.637 (s, 2C, NCH_2), 47.775 (s, 1C, CH_3), 31.607 (s, 2C, PCH_2). MALDI-MS (TOF-TOF): Observed $C_{33}H_{39}ClF_5NO_4P_3Pd$ (without one fluorine) at m/z = 949.4, calculated 949.6.

Notes and references

References

(1) Pehn, R.; Viertl, W.; Bendig, M.; Roithmeyer, H.; Pann, J.; Ehrmann, K.; Mueller, T.; Kopacka, H.; Brüggeller, P. Synthesis of various PNP ligands. *European Journal of Inorganic Chemistry*, manuscript in preparation.

(2) Bianchini, C.; Meli, A.; Oberhauser, W.; Segarra, A. M.; Claver, C.; Suarez, E. J. G. CO-ethylene copolymerization reactions in different reaction media catalyzed by palladium(II) complexes with chelating diphosphines bearing ortho-methoxy-substituted aryl groups. *Journal of Molecular Catalysis A: Chemical* **2007**, *265*, 292–305, DOI: 10.1016/j.molcata.2006.10.035.